

Stable Carbene and Diazoalkane Complexes of the Same Complex System. Synthesis, Structure, and Reactivity of PNP–Ru(II) Fluorenylidene and Diazo fluorene Complexes

Jing Zhang,[†] Mark Gandelman,[†] Linda J. W. Shimon,[‡] and David Milstein^{*†}

Department of Organic Chemistry and Unit of Chemical Research Support, The Weizmann Institute of Science, Rehovot, 76100, Israel

Received April 2, 2008

The choice of synthetic methodology leads to either carbene or diazoalkane complexes of the same system. Thus, treatment of RuCl₂(PPh₃)₃ with 9-diazo fluorene followed ^tBu-PNP (^tBu-PNP = 2,6-bis(di-*tert*-butylphosphinomethyl)pyridine) resulted in loss of dinitrogen and formation of the Ru(II) fluorenylidene complex **1**. On the other hand, treatment of the ^tBu-PNP Ru(II) dinitrogen complex **4** with 9-diazo fluorene resulted in the formation of η^1 -diazo fluorene Ru(II) complex **5**, in which the diazo unit remains intact. The cationic Ru(II) carbene complex **2** was obtained by the reaction of **1** with 1 equiv of AgBF₄ or HBF₄. Chloride dissociation to form a 16-e cationic carbene complex **3** took place also upon refluxing of **1** in toluene. The five-coordinated, unsaturated, charge-neutral diiodide Ru(II) complex **6** was obtained by reaction of **4** with NaI. Complex **6** is stabilized by a C–H agostic interaction, as observed by X-ray crystallography. Reaction of **4** with NaBEt₃H followed by 9-diazo fluorene resulted in a novel η^1 -diazofluorene Ru(II) complex **7**, accompanied by the migration of one hydrogen atom from the metal center to the coordinated nitrogen atom of the diazenofluorene unit. Heating complex **7** at 65 °C resulted in sp² C–H activation followed by elimination of dihydrogen to form the chelated, β -carbon coordinated diazenofluorene ruthenium complex **8**. Complexes **1**, **2**, **5**, **6**, and **8** were structurally characterized by X-ray crystallography.

Introduction

Diazoalkanes are an important class of reagents in organometallic chemistry,¹ useful in metal–carbene synthesis,^{1a,2,3} cyclopropanation,⁴ and C–H activation.⁴ Metal carbenes are useful metathesis catalysts.⁵ The direct reaction of diazoalkanes with transition metals can result in formation of a diazoalkane complex or in N₂ loss to form a metal–carbene complex. The diazoalkane ligand can coordinate to a single metal center either end-on through the terminal nitrogen atom⁶ or side-on through

the N–N or C–N atoms.⁷ It can also coordinate to more than one metal in various bridging modes.⁸ As we have shown experimentally and computationally,⁹ formation of a carbene complex involves intermediacy of a η^2 -C–N diazoalkane intermediate (and not a terminally bound diazoalkane complex). Because of steric constraints for formation of this intermediate, a carbene complex is not formed in sterically hindered systems. On the other hand, Schrock-type metal carbene complexes normally require steric protection to prevent decomposition pathways. This situation results in a “steric window” that can kinetically allow formation of the carbene from the diazoalkane substrate, while stabilizing the product carbene. Stable carbene and diazoalkane complexes of the same system are very rare.¹⁰

Transition metal complexes based on the bulky, electron-rich pincer ligands ^tBu-PNP (2,6-bis(di-*tert*-butylphosphinomethyl)pyridine)^{11,12} and ^tBu-PNN (2-(di-*tert*-butylphosphinomethyl)-6-dimethylaminopyridine)¹³ have found interesting application

* Corresponding author. E-mail: david.milstein@weizmann.ac.il. Fax: 972-8-9344142.

[†] Department of Organic Chemistry.

[‡] Unit of Chemical Research Support.

(1) (a) Herrmann, W. A. *Angew. Chem., Int. Ed. Engl.* **1978**, *17*, 800. (b) Mizobe, Y.; Ishii, Y.; Hidai, M. *Coord. Chem. Rev.* **1995**, *139*, 281. (c) Putala, M.; Lemenovskii, D. A. *Russ. Chem. Rev.* **1994**, *63*, 197.

(2) Roper, W. R. *J. Organomet. Chem.* **1986**, *300*, 167.

(3) Werner, H. J. *Organomet. Chem.* **1995**, *500*, 331.

(4) (a) Padwa, A.; Weingarten, M. D. *Chem. Rev.* **1996**, *96*, 223. (b) Doyle, M. P.; Forbes, D. C. *Chem. Rev.* **1998**, *98*, 911. (c) Davies, H. M. L.; Panaro, S. A. *Tetrahedron* **2000**, *56*, 4871. (d) Davies, H. M. L.; Antoulinakis, E. G. *J. Organomet. Chem.* **2001**, *617–618*, 47.

(5) For some reviews see: (a) Fürstner, A. *Angew. Chem., Int. Ed.* **2000**, *39*, 3012–3043. (b) Trnka, T. M.; Grubbs, R. H. *Acc. Chem. Res.* **2001**, *34*, 18–29. (c) Hoveyda, A. H.; Schrock, R. R. *Chem.–Eur. J.* **2001**, *7*, 945–950.

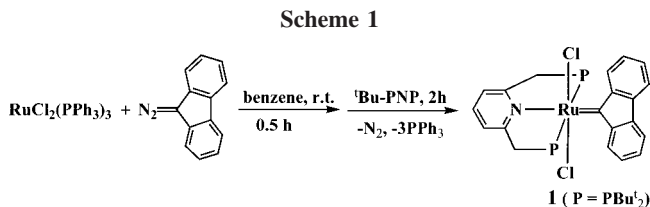
(6) (a) Sutton, D. *Chem. Rev.* **1993**, *93*, 995. (b) Dartiguenave, M.; Menu, M. J.; Deydier, E.; Dartiguenave, Y.; Siebald, H. *Coord. Chem. Rev.* **1998**, *178–180*, 623. (c) Schramm, K. D.; Ibers, J. A. *Inorg. Chem.* **1980**, *19*, 2435. (d) Schramm, K. D.; Ibers, J. A. *Inorg. Chem.* **1980**, *19*, 1231. (e) Schramm, K. D.; Ibers, J. A. *J. Am. Chem. Soc.* **1978**, *100*, 2932. (f) Herrmann, W. A. *J. Organomet. Chem.* **1975**, *85*, C25. (g) Hidai, M.; Mizobe, Y.; Sato, M.; Kodama, J.; Uchida, Y. *J. Am. Chem. Soc.* **1978**, *100*, 5470.

(7) (a) Nakamura, A.; Yoshida, T.; Cowei, M.; Otsuka, S.; Ibers, J. A. *J. Am. Chem. Soc.* **1977**, *99*, 2108. (b) Schramm, K. D.; Ibers, J. A. *Inorg. Chem.* **1980**, *19*, 2441. (c) Otsuka, S.; Nakamura, A.; Koyama, T.; Tatsuno, Y. *Justus Liebigs Ann. Chem.* **1975**, 626. (d) Nakamura, A.; Aotake, M.; Otsuka, S. *J. Am. Chem. Soc.* **1974**, *96*, 3456. (e) Polse, J. L.; Kaplan, A. W.; Andersen, R. A.; Bergman, R. G. *J. Am. Chem. Soc.* **1998**, *120*, 6316.

(8) (a) Herrmann, W. A.; Schweizer, I. Z. *Naturforsch., B: Anorg. Chem., Org. Chem.* **1978**, *33B*, 911. (b) Herrmann, W. A.; Ziegler, M. L.; Weidenhammer, K. *Angew. Chem., Int. Ed. Engl.* **1976**, *15*, 368. (c) Herrmann, W. A.; Bell, L. K. *J. Organomet. Chem.* **1982**, *239*, C4. (d) Messerle, L.; Curtis, M. D. *J. Am. Chem. Soc.* **1980**, *102*, 7789. (e) Gao, Y.; Jennings, M. C.; Puddephatt, R. J. *Organometallics* **2001**, *20*, 3500.

(9) Cohen, R.; Rybtchinski, B.; Gandelman, M.; Rozenberg, H.; Martin, J. M. L.; Milstein, D. *J. Am. Chem. Soc.* **2003**, *125*, 6532.

(10) (a) Schwab, P.; Mahr, N.; Wolf, J.; Werner, H. *Angew. Chem., Int. Ed. Engl.* **1993**, *32*, 1480. (b) Werner, H.; Schwab, P.; Bleuel, E.; Mahr, N.; Steinert, P.; Wolf, J. *Chem.–Eur. J.* **1997**, *3*, 1375.



in C–H activation reactions and in catalysis. Following our continued interest in pyridine-based pincer complexes, we have studied the reactivity of 9-diazofluorene with ^tBu-PNP ruthenium complexes. Interestingly, stable Ru(II) carbene and diazofluorene complexes were formed in the same system depending on the synthetic methods employed.

Results and Discussion

Synthesis and Characterization of the Diazofluorene-Derived Carbene Complex, [Ru{=C(C₁₂H₈)}Cl₂(^tBu-PNP)], **1.** According to a report by Grubbs, no reaction was observed between RuCl₂(PPh₃)₃ and 9-diazofluorene at room temperature,¹⁴ although various other diazoalkane compounds reacted with this complex to give ruthenium carbenes. We have observed that when RuCl₂(PPh₃)₃ was treated with 1 equiv of 9-diazofluorene at room temperature for 0.5 h, followed by reaction with 1 equiv of ^tBu-PNP for 2 h, the Ru(II) carbene complex **1** was formed in 83% isolated yield (Scheme 1). The ³¹P{¹H} NMR spectrum of **1** exhibits a singlet at 49.5 ppm, indicating that the two phosphorus atoms of the ^tBu-PNP complexes are magnetically equivalent. The 9-fluorene carbene group is clearly evidenced by the ¹³C{¹H} NMR signal at 316.8 ppm, which is at a comparable chemical shift to that reported for the carbene carbon of the Rh(III) fluorenylidene complex *trans*-[RhCl{=C(C₁₂H₈)}(SbiPr₃)₂] (309.3 ppm).^{10b} At 298 K, the ¹H NMR spectrum of **1** exhibits one triplet at 0.94 ppm (*J*_{PH} = 6.0 Hz, 18H) and three very broad peaks at 1.10 (6H), 1.40 (6H), and 2.15 ppm (6H), which can be assigned to the 36 protons of the four *tert*-butyl groups of ^tBu-PNP. Upon cooling, the three broad signals became sharp, and at 228 K two triplet signals at 0.98 (6H, *J*_{PH} = 5.5 Hz) and 2.13 (6H, *J*_{PH} = 6.0 Hz)

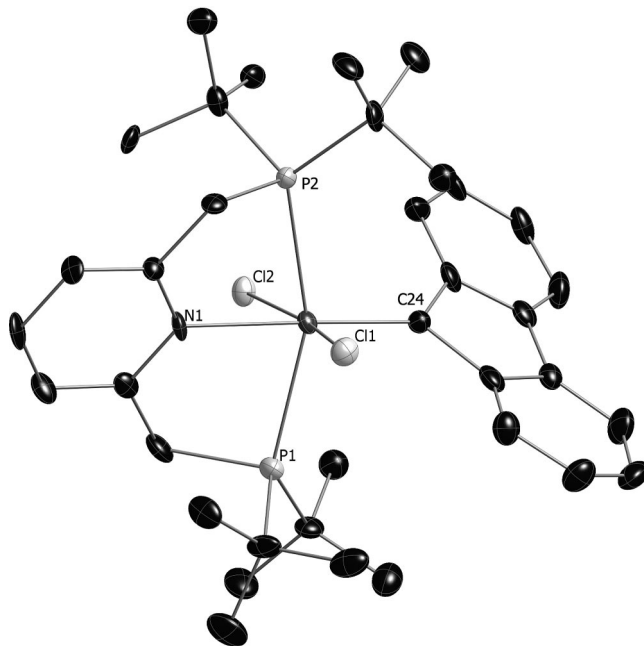


Figure 1. ORTEP diagram of a molecule of complex **1** with the thermal ellipsoids at the 50% probability level. All hydrogen atoms were omitted for clarity.

and one singlet at 1.42 ppm (6H) were observed. These ¹H NMR data may indicate that two of the ^tBu groups experience hindered rotation about the P–C bond due to steric interaction with the fluorenylidene ligand. Complex **1** is stable at room temperature for several weeks in various solvents (e.g., THF, benzene, toluene) without observable decomposition.

Orange, single crystals suitable for X-ray diffraction were obtained by slow evaporation of a diethyl ether solution of **1** at –32 °C. The crystal structure of **1** (Figure 1) displays a distorted octahedral geometry around the metal center. The fluorenylidene unit is bound to the ruthenium center *trans* to the nitrogen atom of the ^tBu-PNP ligand (N1–Ru1–C24, 177.9(4)°). The two chloride ligands are coordinated *trans* to each other. The bond distance of Ru1–C24 (1.936(9) Å) is slightly longer than the one reported for the ruthenium indenylidene complex [(IPi)(PCy₃)Cl₂Ru(3-phenylindenylid-1-ene)] (IPi = 1,3-bis(2,6-diisopropylphenyl)imidazol-2-ylidene) (1.861(4) Å).¹⁵ The dihedral angle between the fluorene plane and the coordination plane defined by P1, N1, P2, and Ru1 is 61.7°, minimizing steric interaction between the fluorenylidene ligand and the phosphine and chloride ligands.

Synthesis and Characterization of the Fluorenylidene Complexes [Ru{=C(C₁₂H₈)}(^tBu-PNP)Cl][BF₄] (2**) and [Ru{=C(C₁₂H₈)}(^tBu-PNP)Cl][Cl] (**3**).** Treatment of complex **1** with 1 equiv of AgBF₄ in THF resulted in formation of the cationic Ru(II) fluorenylidene complex **2** in almost quantitative yield (Scheme 2). The ³¹P{¹H} NMR spectrum of **2** exhibits a singlet at 67.6 ppm, representing a downfield shift of 18 ppm relative to that of complex **1**. A signal at 299.9 ppm in the ¹³C{¹H} NMR spectrum of **2** is assigned to the coordinated carbon of the fluorenylidene group, which represents an upfield shift of 17 ppm relative to that of complex **1**. As expected, the ¹H NMR spectrum exhibits two triplets at 0.84 and 1.33 ppm for the *tert*-butyl protons and two double triplets at 3.53 and 4.30 ppm for the methylene protons of the ^tBu-PNP ligand,

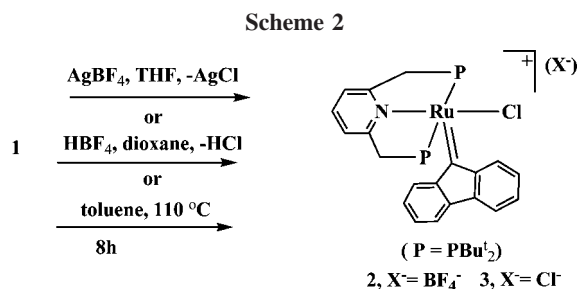
(11) (a) Hermann, D.; Gandelman, M.; Rozenberg, H.; Shimon, L. J. W.; Milstein, D. *Organometallics* **2002**, *21*, 812. (b) Ben-Ari, E.; Gandelman, M.; Rozenberg, H.; Shimon, L. J. W.; Milstein, D. *J. Am. Chem. Soc.* **2003**, *125*, 4714. (c) Zhang, J.; Gandelman, M.; Shimon, L. J. W.; Rozenberg, H.; Milstein, D. *Organometallics* **2004**, *23*, 4026. (d) Ben-Ari, E.; Cohen, R.; Gandelman, M.; Shimon, L. J. W.; Martin, J. M. L.; Milstein, D. *Organometallics* **2006**, *25*, 3190. (e) Ben-Ari, E.; Leituss, G.; Shimon, L. J. W.; Milstein, D. *J. Am. Chem. Soc.* **2006**, *128*, 15390. (f) Zhang, J.; Leituss, G.; Ben-David, Y.; Milstein, D. *Angew. Chem., Int. Ed.* **2006**, *45*, 1113. (g) Feller, M.; Karton, A.; Leituss, G.; Martin, J. M. L.; Milstein, D. *J. Am. Chem. Soc.* **2006**, *128*, 12400. (h) Precht, M. H.G.; Holscher, M.; Ben-David, Y.; Theyssen, N.; Loschen, R.; Milstein, D.; Leitner, W. *Angew. Chem., Int. Ed.* **2007**, *46*, 2269.

(12) (a) Kawatsura, M.; Hartwig, J. F. *Organometallics* **2001**, *20*, 1960. (b) Stambuli, J. P.; Shaun, S. R.; Shaughnessy, K. H.; Hartwig, J. F. *J. Am. Chem. Soc.* **2001**, *123*, 2677. (c) Gibson, D. H.; Pariya, C.; Mashuta, M. S. *Organometallics* **2004**, *23*, 2510. (d) Kloek, S. M.; Heinekey, D. M.; Goldberg, K. I. *Organometallics* **2006**, *25*, 3007. (e) Benito-Garagori, D.; Becker, E.; Wiederman, J.; Lackner, W.; Pollak, M.; Mereiter, K.; Kisala, J.; Kirchner, K. *Organometallics* **2006**, *25*, 1900. (f) Kloek, S. M.; Heinekey, D. M.; Goldberg, K. I. *Angew. Chem., Int. Ed.* **2007**, *46*, 4736. (g) Benito-Garagori, D.; Wiederman, J.; Pollak, M.; Mereiter, K.; Kirchner, K. *Organometallics* **2007**, *26*, 217.

(13) (a) Zhang, J.; Leituss, G.; Ben-David, Y.; Milstein, D. *J. Am. Chem. Soc.* **2005**, *127*, 10840. (b) Zhang, J.; Gandelman, M.; Herrman, D.; Leituss, G.; Shimon, L. J. W.; Ben-David, Y.; Milstein, D. *Inorg. Chim. Acta* **2006**, *359*, 1955. (c) Zhang, J.; Gandelman, M.; Shimon, L. J. W.; Milstein, D. *Dalton Trans.* **2007**, 107. (d) Gunanathan, C.; Ben-David, Y.; Milstein, D. *Science* **2007**, *317*, 790.

(14) Schwab, P.; Grubbs, R. H.; Ziller, J. W. *J. Am. Chem. Soc.* **1996**, *118*, 100.

(15) Jafarpour, L.; Schanz, H.-J.; Stevens, E. D.; Nolan, S. P. *Organometallics* **1999**, *18*, 5416.



indicating lack of a symmetry plane involving the P, N, P, and Ru atoms. It is interesting that complex **2** can also be obtained by treatment of complex **1** with 1 equiv of HBF₄ in good yield (90%). HBF₄ protonates a chloride ligand, releasing HCl, rather than protonating the Ru=C bond. Complex **2** is stable even in the presence of excess HBF₄ in dioxane.

Interestingly, formation of the cationic complex **3**, analogous to **2** but with a chloride counteranion, can be accomplished simply by heating of **1**, reflecting the steric hindrance experienced by complex **1**. Thus, refluxing a toluene solution of **1** at 110 °C for 8 h resulted in formation of **3** in 90% yield (Scheme 2). The ³¹P{¹H} NMR spectrum of **3** is practically the same as that of **2**. As expected, treatment of **3** with 1 equiv of AgBF₄ resulted in its quantitative conversion to complex **2**.

Single crystals of **2** suitable for an X-ray diffraction study were obtained by slow diffusion of diethyl ether into a concentrated THF solution of complex **2**. The crystal structure of **2** (Figure 2) displays a distorted square-pyramidal geometry around the metal center. The four basal atoms (N1, P1, P2, Cl1) are almost coplanar, with an average deviation from planarity of 0.103 Å, and the ruthenium atom is located 0.428 Å out of the basal plane in the direction of the apical atom C24. The chloride ligand is located *trans* to the nitrogen atom of 'Bu-PNP (Cl1–Ru1–N1, 152.5(1)°), and the fluorenylidene unit is coordinated *cis* to the nitrogen atom (N1–Ru1–C24, 98.0(2)°) and *trans* to the vacant coordination site. This geometry is a result of the large *trans* effect of the carbon atom. The Ru=C bond distance, Ru1–C24 (1.877(5) Å), is slightly shorter than the corresponding bond of complex **1** and similar to that reported for the carbene complex [(IPi)(PCy₃)Cl₂Ru(3-phenylindenylidene)] (1.861(4) Å).¹⁵ The bond distance of Ru1–N1 (2.100(5) Å) is significantly shorter than that of complex **1** (2.191(7) Å),

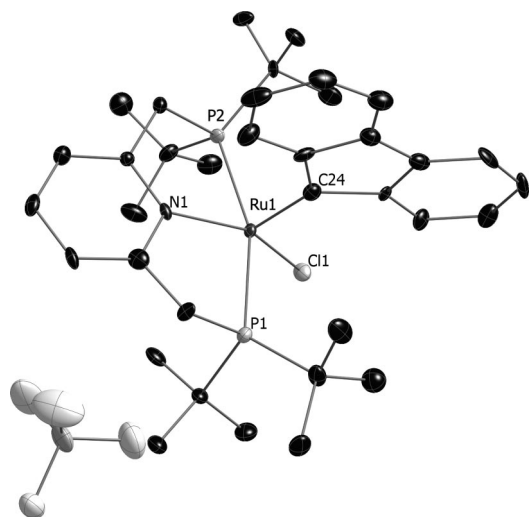


Figure 2. ORTEP diagram of a molecule of complex **2** with the thermal ellipsoids at the 50% probability level. All hydrogen atoms were omitted for clarity.

as a result of the larger *trans* effect of carbon relative to the chloride. The dihedral angle between the fluorene plane and the coordination plane defined by P1, N1, P2, and Cl1 is 85.9°, which is preferred sterically.

It was hoped that the unsaturated fluorenylidene Ru(II) complexes would show metathesis reactivity. However, upon treatment of complex **2** with allylbenzene or norbornene both at room temperature (in dichloromethane) and at high temperature (90 °C, in toluene), no metathesis products were observed and complex **2** was recovered in almost quantitative yield. This might be a result of the steric environment of the Ru(II) center, which hindered olefin coordination.

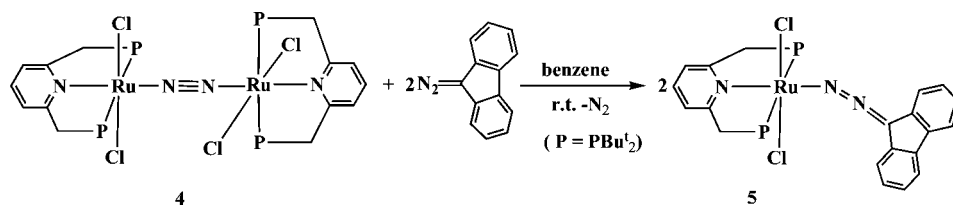
Synthesis and Characterization of the PNP–Ru(II) Diazo fluorene Complex Ru{N₂=C(C₁₂H₈)}(PNP)Cl₂, **5.** As we reported, the dinitrogen complex **4** was obtained by refluxing RuCl₂(PPh₃)₃ with 1 equiv of PNP in THF.^{11c} Interestingly, treatment of this complex with 2 equiv of 9-diazo fluorene in benzene at room temperature did not result in formation of the carbene complex, but rather the diazo fluorene complex **5** was formed in 91% yield (Scheme 3). The ³¹P{¹H} NMR spectrum of **5** exhibits a singlet at 65.8 ppm, similar to that of complex **4** (65.0 ppm). The signal at 67.8 ppm in the ¹³C{¹H} NMR spectrum of **5** is assigned to C-9 of the fluorene unit, which is connected to the diazo group. The lack of a signal around 300 ppm indicates the absence of a carbene moiety. A strong absorption at 2054 cm⁻¹ in the IR spectrum of **5** indicates that the diazo fluorene is coordinated to the ruthenium center in a η¹-N₂C mode (compared to the η²-diazo fluorene complex [Ni('BuNC)₂(diazo fluorene)], ν_(N₂C) = 1509 cm⁻¹).^{7a} This typical feature of the position of the ν(N₂C) vibration appears at a significantly higher wavenumber than that of a reported rhodium η¹-N₂C coordinated diazo fluorene complex *trans*-[RhCl(N₂CC₁₂H₈)(PiPr₃)₂]¹⁶ (1915 cm⁻¹).

Single crystals of complex **5** suitable for X-ray diffraction were obtained by slow diffusion of pentane into a concentrated toluene solution of **5** at -32 °C. The crystal structure of **5** (Figure 3) displays a distorted octahedral geometry around the metal center. The diazo fluorene unit is bound to the Ru(II) center via the terminal nitrogen atom *trans* to the nitrogen atom of the 'Bu-PNP ligand (N1–Ru–N2, 174.1(1)°) and possesses a severely "bent" configuration with a Ru1–N1–N3 angle of 158.3(2)°, in contrast to the reported Rh(I) complex *trans*-[RhCl(N₂CC₁₃H₈O)(PiPr₃)₂]¹⁶ in which the Rh–N–N angle is 173.7(5)°. The two chloride ligands are *trans* to each other, forming a Cl1–Ru–Cl2 axis with an angle of 174.81(3)°. The bond distance of N1–N3 (1.151(3) Å) is almost identical to the corresponding bond of *trans*-[RhCl(N₂CC₁₃H₈O)(PiPr₃)₂]¹⁶ (1.150(6) Å) and lies between an N–N double and triple bond.¹⁷ It is noted that the two chloride ligands and the two phosphorus atoms of the 'Bu-PNP are bound to the metal center in an asymmetric mode. Thus, the bond distance of Ru1–Cl2 (2.398(1) Å) is shorter than Ru1–Cl1 (2.425(1) Å), while the Ru1–P1 bond (2.423(1) Å) is shorter than Ru1–P2 (2.456(1) Å). In contrast, the Ru–Cl bond lengths in complex **1** are almost equal (2.414(3) and 2.416(3) Å), as are the Ru–P bond lengths (2.451(3) and 2.453(3) Å). The dihedral angle between the fluorene plane and the coordination plane defined by P1, N2, P2, and Ru(1) is 67.7°. Regarding the bonding mode of the diazo fluorene unit, it is noted that in the related nickel complex

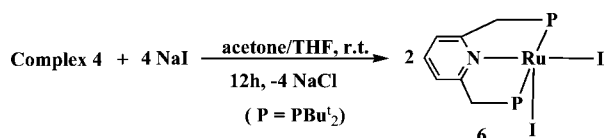
(16) Werner, H.; Mahr, N.; Wolf, J.; Fries, A.; Laubender, M.; Bleuel, E.; Garde, R.; Lahuerta, P. *Organometallics* **2003**, *22*, 3566.

(17) Wells, A. F. *Structural Inorganic Chemistry*, 5th ed.; Clarendon Press: Oxford, 1984; Chapter 18.

Scheme 3



Scheme 4



[Ni(^tBuNC)₂(diazofluorene)] the 9-diazafluorene is coordinated side-on, and thus both nitrogen atoms are linked to the metal center.^{7a}

Few systems are known in which both the carbene and the diazo complexes are stable,¹⁰ and it was of interest to us to see if the diazo complex can be converted into the carbene complex. Heating complex **5** at high temperature (for example, in toluene at 110 °C for 12 h) did not result in denitrogenation to the carbene, and abstracting the chloride ligand from **5** with AgBF₄ did not lead to the carbene either. Apparently, the steric bulk of the ^tBu groups prevents rearrangement of the terminally bound diazo fluorene to the η²-C–N diazo fluorene intermediate, which is probably required for N₂ expulsion and carbene formation.⁹ The importance of steric factors was clearly demonstrated by Werner, who reported that reaction of RhCl(C₂H₄)(PⁱPr₃)₂ with Ph₂CN₂ resulted in the diazo complex RhCl(N₂CPh₂)(PⁱPr₃)₂, while reaction of the analogous complex of the less sterically demanding (smaller cone angle) SbⁱPr₃ ligand produced the metallacarbene RhCl(=CPh₂)(SbⁱPr₃)₂, which was subsequently transformed into RhCl(N₂CPh₂)(PⁱPr₃)₂ by ligand exchange.^{10a}

Synthesis and Characterization of the Diiodide Complex RuI₂(^tBu-PNP), 6. Treatment of complex **4** with 4 equiv of NaI in a mixture of acetone and THF (1:1, v/v) resulted in the formation of complex **6** as a dark green solid in 80% yield (Scheme 4). The ³¹P{¹H} NMR spectrum of **6** exhibits a singlet at 45.0 ppm. The ¹H NMR spectrum of **6** exhibits two broad

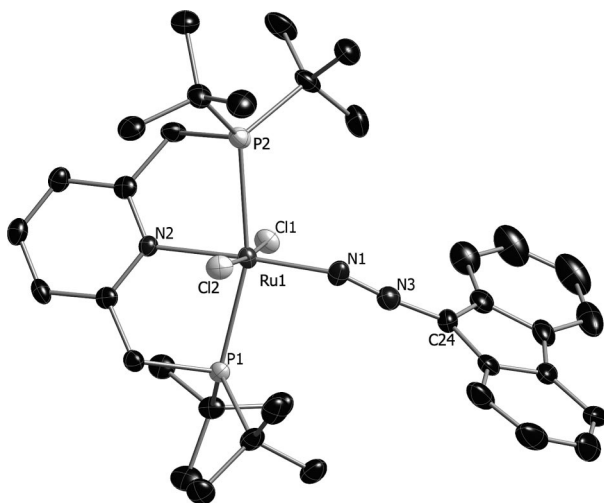


Figure 3. ORTEP diagram of a molecule of complex **5** with the thermal ellipsoids at the 50% probability level. All hydrogen atoms are omitted for clarity.

Table 1. Selected Bond Distances (Å) and Angles (deg) for Complex 1

Ru1–N1	2.191(7)	Ru1–Cl1	2.414(3)
Ru1–Cl2	2.416(3)	Ru1–P1	2.453(3)
Ru1–P2	2.450(3)	Ru1–C24	1.936(9)
N1–Ru1–C24	177.9(4)	Cl1–Ru1–Cl2	169.3(1)
P1–Ru1–P2	157.2(1)	Cl1–Ru1–C24	96.7(3)
Cl2–Ru1–C24	94.0(3)	P1–Ru1–C24	99.8(3)
P2–Ru1–C24	102.9(3)	N1–Ru1–P1	78.5(2)
P2–Ru1–N1	78.7(2)	N1–Ru1–Cl1	84.6(2)
Cl2–Ru1–N1	84.7(2)	P1–Ru1–Cl1	90.0(1)
P1–Ru1–Cl2	88.7(1)	P2–Ru1–Cl1	87.9(1)
P2–Ru1–Cl2	89.2(1)		

Table 2. Selected Bond Distances (Å) and Angles (deg) for Complex 2

Ru1–N1	2.100(5)	Ru1–Cl1	2.400(2)
Ru1–C24	1.877(5)	Ru1–P1	2.418(2)
Ru1–P2	2.409(2)		
N1–Ru1–C24	98.0(2)	Cl1–Ru1–C24	109.5(2)
P1–Ru1–P2	160.5(1)	P1–Ru1–C24	96.4(2)
P2–Ru1–C24	97.5(2)	N1–Ru1–P1	82.4(1)
P2–Ru1–N1	82.2(1)	N1–Ru1–Cl1	152.5(1)
P1–Ru1–Cl1	94.1(1)	P2–Ru1–Cl1	94.0(1)

Table 3. Selected Bond Distances (Å) and Angles (deg) for Complex 5

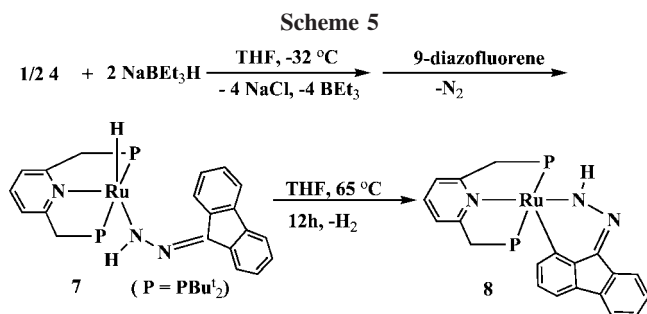
Ru1–N1	1.898(3)	Ru1–N2	2.078(2)
Ru1–Cl1	2.425(1)	Ru1–Cl2	2.398(1)
Ru1–P1	2.413(1)	Ru1–P2	2.456(1)
N1–N3	1.151(3)	N3–C24	1.334(4)
N1–Ru1–N2	174.1(1)	Cl1–Ru1–Cl2	174.81(3)
P1–Ru1–P2	162.63(3)	N1–Ru1–Cl1	88.5(1)
N1–Ru1–Cl2	96.1(1)	N1–Ru1–P1	94.7(1)
P2–Ru1–N1	102.7(1)	N2–Ru1–P2	80.9(1)
N2–Ru1–P1	81.8(1)	N2–Ru1–Cl1	86.9(1)
N2–Ru1–Cl2	88.7(1)	P1–Ru1–Cl1	93.21(3)
P1–Ru1–Cl2	88.80(3)	P2–Ru1–Cl1	87.50(3)
P2–Ru1–Cl2	89.16(3)	Ru1–N1–N3	158.3(3)
N1–N3–C24	170.1(3)		

Table 4. Selected Bond Distances (Å) and Angles (deg) for Complex 6

Ru3–N1	2.077(3)	Ru3–I1	2.743(1)
Ru3–I2	2.687(1)	Ru3–P4	2.318(1)
Ru3–P5	2.411(1)		
N1–Ru3–I1	177.1(1)	N1–Ru3–I2	84.8(1)
P4–Ru3–P5	162.56(4)	N1–Ru3–P4	83.9(1)
N1–Ru3–P5	82.6(1)	I1–Ru3–P4	98.07(3)
I1–Ru3–P5	95.08(3)	I1–Ru3–I2	97.36(2)
I2–Ru3–P4	91.43(3)	I2–Ru3–P5	98.22(4)

singlets at 0.71 and 1.68 ppm for the *tert*-butyl protons and one broad triplet at 4.30 ppm for the methylene protons.

Dark green single crystals suitable for the X-ray analysis of **6** were obtained by slow diffusion of diethyl ether into a concentrated THF solution of **6**. Selected bond distances and bond angles for complex **6** are listed in Table 4. The coordination geometry around the ruthenium atom is approximately octahedral, with one coordination site occupied by an agostic C–H bond of a ^tBu group (Figure 4). One iodide atom is



coordinated *trans* to the pyridinic nitrogen (I1–Ru–N1 177.1(1) $^\circ$) and *cis* to another iodide atom (I1–Ru–I2 97.36(2) $^\circ$). The γ -agostic interaction C15–H15c \cdots Ru is indicated by the geometric parameters of ^tBu–PNP. The Ru3–P4–C13 (97.8(1) $^\circ$) and P4–C13–C15 (101.2(3) $^\circ$) angles are significantly smaller than the corresponding Ru3–P5–C17 (116.0(1) $^\circ$) and P5–C17–C23 (109.1(3) $^\circ$), respectively. It is noted that the bond distance of Ru3–P4 (2.318 (1) Å) is significantly shorter than that of Ru3–P5 (2.411(1) Å) due to a contraction in the Ru–P4–C13–C15–H15c cycle. The Ru–C15 separation of 2.665 Å is shorter than that reported for the complex RuCl₂(POP–Bu^t) (POP–Bu^t = (^tBu₂PCH₂CH₂)₂O) (2.845 Å).¹⁸

Synthesis and Characterization of [RuH(N₂)(HNNC₁₃H₈)(^tBu–PNP)] 7. Upon reaction of the dinitrogen complex **4** with 4 equiv of NaBEt₃ in THF at –32 °C, an unstable Ru(II) dihydride complex formed. The ³¹P{¹H} NMR spectrum of this complex exhibits a singlet at 102.1 ppm and the ¹H NMR spectrum shows a triplet at –4.60 ppm (*J*_{PH} = 22.5 Hz, 2H), suggesting formation of a Ru(II) dihydride or Ru(0) dihydrogen complex. The spin–lattice relaxation time of the signal at –4.60 ppm (*t*₁ = 1.20 s) indicates that the complex is a *trans*-Ru(II) dihydride. This complex is stable at room temperature only for a few hours and decomposes to several unidentified complexes. Attempts to isolate it resulted in complete decomposition to a mixture of unidentified complexes.

Treatment of this ruthenium complex in THF with 1 equiv of 9-diazafluorene at room temperature resulted in a quick color change of the solution from yellow to dark orange. A stable orange complex, **7**, was obtained in 57% yield (Scheme 5). ³¹P{¹H} NMR of **7** shows a singlet at 81.0 ppm, representing an upfield shift of 21 ppm relative to the ruthenium dihydride complex. The presence of one hydride coordinated to the Ru(II)

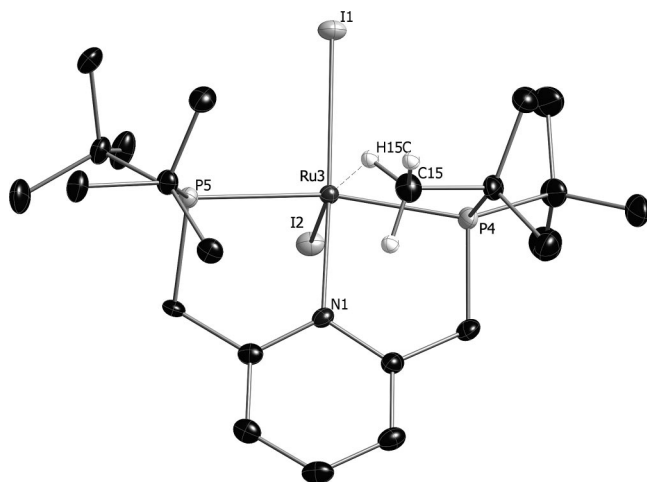


Figure 4. ORTEP diagram of a molecule of complex **6** with the thermal ellipsoids at the 50% probability level. All hydrogen atoms, except for agostic C–H, are omitted for clarity.

Table 5. Selected Bond Distances (Å) and Angles (deg) for Complex **8**

Ru1–N1	2.118(3)	Ru1–N2	2.037(3)
Ru1–C24	1.997(4)	Ru1–P2	2.365(1)
Ru1–P3	2.330(1)	N2–N3	1.306(5)
N2–H2	0.81(5)	N3–C35	1.347(5)
N1–Ru1–N2	173.4(1)	N1–Ru1–C24	93.7(2)
N1–Ru1–P2	82.6(1)	N1–Ru1–P3	83.1(1)
N2–Ru1–C24	92.9(2)	N2–Ru1–P2	95.6(1)
P3–Ru1–N2	97.8(1)	P2–Ru1–C24	97.4(1)
P3–Ru1–C24	91.3(1)	P2–Ru1–P3	163.71(4)
Ru1–N2–N3	133.7(3)	N2–N3–C35	116.9(3)

center is confirmed by the ¹H NMR spectrum, which exhibits one triplet peak at –12.01 ppm with *J*_{PH} = 19.0 Hz. The existence of two triplet peaks at 1.28 and 1.37 ppm for the *tert*-butyl protons, one double triplet peak at 3.45 ppm, and one broad doublet peak at 3.89 ppm for the methylene protons indicate lack of a symmetry plane involving the P, N, and P atoms. A broad singlet peak at 9.15 ppm can be assigned to the NH of α -protonated diazo fluorene, which is similar to other observations of closely related aryldiazene complexes.¹⁹ The IR spectrum of **7** exhibits a band at 3205 cm^{–1}, which is typical for an N–H moiety. Complex **7** presents a rare example in which a hydride ligand migrates from a metal center to the α -nitrogen of the coordinated diazo compound. Another example of the iridium complex [IrCl₂(HN₂C(C(O)Ph)₂)(PPh₃)₂] was reported by Cowie and co-workers.²⁰ We have also reported a PCP Rh complex that underwent intramolecular hydride migration to a C-coordinated diazo ligand.²¹

Synthesis and Characterization of [Ru(HNNC₁₃H₇)(PNP)] 8. Heating complex **7** in dry THF at 65 °C for 12 h results in the color change of the solution from orange to dark red, and the new complex **8** was formed in 90% yield (Scheme 5). The ³¹P{¹H} NMR spectrum of **8** shows a singlet peak at 58.5 ppm, representing an upfield shift of 22.5 ppm relative to complex **7**. A broad singlet peak at 8.50 ppm in the ¹H NMR, which can be assigned to the N–H moiety, and the singlet peak at 67.9 ppm in the ¹³C{¹H} NMR of **8** indicate the existence of the coordinated HN₂ moiety of diazenofluorene, which is similar to that of the complex **7**. The ¹H NMR of **8** exhibits seven protons (four groups of doublet peaks and three groups of triplet peaks) for the fluorine unit, and a singlet peak at 158.4 ppm is observed in ¹³C{¹H} NMR, indicating the formation of Ru–C (1-position of fluorine).

Single crystals suitable for the X-ray diffraction were obtained by slow diffusion of pentane to the concentrated THF solution of **8**. Selected bond distances and bond angles for complex **8** are listed in Table 5.

The X-ray structure of **8** exhibits a distorted square-pyramidal geometry around the ruthenium center, with the *cis* angles in the range 82.6(1) $^\circ$ to 97.8(1) $^\circ$ (Figure 5) and C24 located in an apical position with a Ru1–C24 bond distance of 1.997(4) Å. The bond distance of Ru1–N2 (2.037(3) Å) is longer than that of complex **5** (1.898(3) Å), while the distance of N2–N3 (1.306(5) Å) is significantly longer than that of complex **5** (1.151(4) Å), clearly indicating the formation of a diazenic

(18) Major, Q.; Lough, A. J.; Gusev, D. G. *Organometallics* **2005**, *24*, 2492.

(19) (a) Gilchrist, A. B.; Sutton, D. J. *Chem. Soc., Dalton Trans.* **1977**, 677. (b) Parshall, G. W. *J. Am. Chem. Soc.* **1967**, *89*, 1822. (c) Toniolo, L.; Eisenberg, R. *J. Chem. Soc., Chem. Commun.* **1971**, 455. (d) Haymore, B. L.; Ibers, J. A. *J. Am. Chem. Soc.* **1975**, *97*, 5369.

(20) Cowie, M.; Loeb, S. J.; Mckeer, I. R. *Organometallics* **1986**, *5*, 854.

(21) Frech, C. M.; Shimon, L. J. W.; Milstein, D. *Chem.–Eur. J.* **2007**, *13*, 7501.

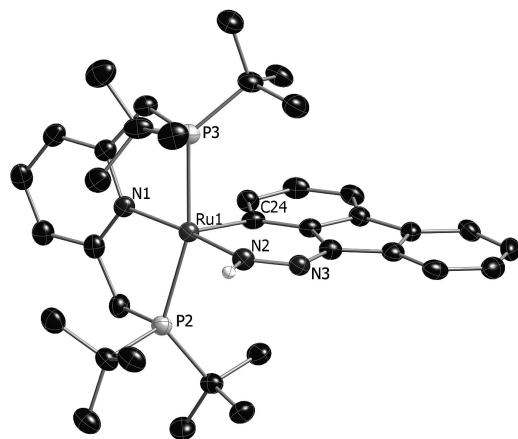


Figure 5. ORTEP diagram of a molecule of complex **8** with the thermal ellipsoids at the 50% probability level. All hydrogen atoms are omitted for clarity.

anionic ligand (HNN). Complex **8** was formed from complex **7** by a β -aryl C–H activation of the fluorene ligand followed by elimination of dihydrogen, forming a six-membered metallacycle. As a result of the ring formation, the angles Ru1–N2–N3 ($133.7(3)^\circ$) and N2–N3–C35 ($116.9(3)^\circ$) are contracted considerably as compared with the corresponding angles of complex **5** ($158.3(3)^\circ$ and $170.1(3)^\circ$, respectively) and are similar to those observed in the case of the diazenic metal complex $[\text{IrCl}_2(\text{HN}_2\text{C}(\text{C}(\text{O})\text{Ph}_2)_2)(\text{PPh}_3)_2]$ ¹⁸ ($131(2)^\circ$ and $121(2)^\circ$, respectively). The bond distance of N2–N3 ($1.306(5) \text{ \AA}$) is longer than the corresponding bond of the coordinated diazo fluorene in complex **5** ($1.151(4) \text{ \AA}$) and in the complexes $[\text{IrCl}_2(\text{HN}_2\text{C}(\text{C}(\text{O})\text{Ph}_2)_2)(\text{PPh}_3)_2]$ ($1.25(2) \text{ \AA}$)¹⁹ and $[(\text{dtbpm}-\kappa^2\text{P})\text{Pt}\{\text{NHNC}(\text{CO}_2\text{Me})_2-\kappa\text{N},\kappa\text{O}\}](\text{BF}_4^-)$ (dtbpm = bis(di-*tert*-butylphosphino)methane) ($1.289(6) \text{ \AA}$).²² The metal–aryl bond distance of Ru1–C24 ($1.857(5) \text{ \AA}$) is significantly shorter than those of Ru(Ph)Cl(CO)(P^{*t*}Bu₂Me)₂ ($2.0394(4) \text{ \AA}$)²³ and Ru(*p*-tolyl)Cl(CO)(PPh₃)₂ ($2.056(3) \text{ \AA}$).²⁴ The dihedral angle between the fluorene plane and the coordination plane defined by P2, N1, P3, and Ru1 is 96.2° .

Summary. Synthetic pathways leading to either 9-diazo fluorene or fluorenylidene complexes of the same Ru(II) system were developed. Thus, the ruthenium fluorenylidene complex **1**, based on the electron-rich, bulky ligand ^{*t*}Bu-PNP, was prepared by the reaction of RuCl₂(PPh₃)₃ with 9-diazo fluorene followed by reaction with ^{*t*}Bu-PNP. On the other hand, direct reaction of the ^{*t*}Bu-PNP–Ru(II) dinitrogen complex **4** with 9-diazo fluorene resulted in the formation of ^{*t*}Bu-PNP–Ru diazo fluorene complex **5**, in which the diazo unit remained intact and coordinated to the Ru(II) center in a $\eta^1 \text{N}=\text{NR}$ mode. The reason for the different outcome of the two approaches is kinetic, i.e., steric constraints for reaching the transition state required for N₂ loss from the diazoalkane ligand in the case of the bulky complex **4**. Stable, coordinatively unsaturated 16-electron, cationic carbene complex **2** as well as neutral diiodo ruthenium complex **6** were obtained. Complex **6** is stabilized by an agostic C–H interaction. Reaction of the dinitrogen complex **4** with NaHBEt₃ resulted in the formation of an unstable Ru(II) dihydride complex, which reacted with 9-diazo fluorene to form

the ruthenium diazeno fluorene complex **7** as a result of a rare hydride migration to a coordinated nitrogen atom of a diazo ligand. The diazeno fluorene ligand readily underwent intramolecular C–H activation by the Ru(II) center of complex **7**, yielding after H₂ elimination a six-membered diaza-metallacycle.

Experimental Section

General Procedures. All experiments with metal complexes and phosphine ligands were carried out under an atmosphere of purified nitrogen in a Vacuum Atmospheres glovebox equipped with a MO 40-2 inert gas purifier or using standard Schlenk techniques. All solvents were reagent grade or better. All nondeuterated solvents were refluxed over sodium/benzophenone ketyl and distilled under argon atmosphere. Deuterated solvents were used as received. All solvents were degassed with argon and kept in the glovebox over 4 Å molecular sieves. The ligand 2,6-bis(di-*tert*-butylphosphino-methyl)pyridine (^{*t*}Bu-PNP),^{11a} RuCl₂(PPh₃)₃,²⁵ and 9-diazo fluorene²⁶ were prepared according to literature procedures.

¹H, ¹³C, and ³¹P NMR spectra were recorded at 400 or 500, 100 or 126, and 162 or 202 MHz, respectively, using Bruker AMX-400 and AMX-500 NMR spectrometers. ¹H and ¹³C{¹H} NMR chemical shifts are reported in ppm downfield from tetramethylsilane. ³¹P NMR chemical shifts are reported in parts per million downfield from H₃PO₄ and referenced to an external 85% solution of phosphoric acid in D₂O. Abbreviations used in the NMR follow-up experiments: b, broad; s, singlet; d, doublet; t, triplet; q, quartet; m, multiplet; v, virtual. Elemental analysis was performed at Kolbe Laboratorium, Mulheim, Germany.

Synthesis of [Ru(=C(C₁₂H₈))Cl₂(^{*t*}Bu-PNP)], **1.** To a suspension of RuCl₂(PPh₃)₃ (96 mg, 0.1 mmol) in toluene (5 mL) was added 9-diazo fluorene (19 mg, 0.1 mmol) at -32°C , and the mixture was stirred at room temperature for 0.5 h. To the resulting dark yellow solution was added ^{*t*}Bu-PNP (40 mg, 0.1 mmol) followed by stirring for another 2 h at room temperature. The solution was evaporated under vacuum to dryness, and the residue was dissolved in a minimum amount of benzene (2 mL). Pentane (20 mL) was added to precipitate a brown solid, which was extracted with diethyl ether (3 × 5 mL). The combined diethyl ether solutions were slowly evaporated under vacuum, yielding orange microcrystalline **1** (60 mg, 83%).

³¹P{¹H} NMR (THF-*d*₈): 49.5 (s). ¹H NMR (THF-*d*₈, 298 K): 0.94 (t, 18H, *J*_{PH} = 6.0 Hz, P(C(CH₃)₃)), 1.10 (br, 6H, P(C(CH₃)₃)₂), 1.40 (br, 6H, P(C(CH₃)₃)₂), 2.15 (br, 6H, P(C(CH₃)₃)₂), 3.56 (dt, 2H, *J*_{HH} = 15.0 Hz, *J*_{PH} = 4.0 Hz, –CHHP), 4.14 (dt, 2H, *J*_{HH} = 15.0 Hz, *J*_{PH} = 3.3 Hz, –CHHP), 7.06 (t, 2H, *J*_{HH} = 7.5 Hz, fluorine-H2, H7), 7.36 (d, 2H, *J*_{HH} = 7.5 Hz, fluorine-H4, H5), 7.50 (d, 2H, *J*_{HH} = 8.0 Hz, pyridine-H3, H5), 7.59 (t, 2H, *J*_{HH} = 7.5 Hz, fluorine-H3, H6), 7.76 (t, 1H, *J*_{HH} = 8.0 Hz, pyridine-H4), 9.62 (d, 2H, *J*_{HH} = 8.0 Hz, fluorine-H1, H8). ¹H NMR (THF-*d*₈, 228 K): 0.89 (t, 18H, *J*_{PH} = 6.0 Hz, P(C(CH₃)₃)), 0.98 (t, 6H, *J*_{PH} = 5.5 Hz, P(C(CH₃)₃)₂), 1.42 (s, 6H, P(C(CH₃)₃)₂), 2.13 (t, 6H, *J*_{PH} = 6.0 Hz, P(C(CH₃)₃)₂), 3.64 (dt, 2H, *J*_{HH} = 15.0 Hz, *J*_{PH} = 4.0 Hz, –CHHP), 4.00 (d, 2H, br, *J*_{HH} = 15.0 Hz, –CHHP), 7.06 (t, 2H, *J*_{HH} = 7.5 Hz, fluorine-H2, H7), 7.39 (d, 2H, *J*_{HH} = 7.5 Hz, fluorine-H4, H5), 7.55 (d, 2H, *J*_{HH} = 8.0 Hz, pyridine-H3, H5), 7.61 (t, 2H, *J*_{HH} = 7.5 Hz, fluorine-H3, H6), 7.81 (t, 1H, *J*_{HH} = 8.0 Hz, pyridine-H4), 9.58 (d, 2H, *J*_{HH} = 8.0 Hz, fluorine-H1, H8). ¹³C{¹H} NMR (THF-*d*₈, 298 K): 31.3 (s, P(CH(CH₃)₂)₂), 31.7 (s, P(C(CH₃)₃)₂), 37.5 (t, *J*_{PC} = 3.8 Hz, P(C(CH₃)₃)₂), 40.2 (t, *J*_{PC} = 7.5 Hz, CH₂P), 118.3 (s, fluorine-C4, C5), 121.7 (t, *J*_{PC} = 3.8 Hz, pyridine-C3, C5), 128.5 (s, fluorine-C2, C7), 131.5 (s, fluorine-C3, C6), 134.4 (s, fluorine-C1, C8), 138.7 (s, pyridine-C4), 139.8 (s, fluorine-C11, C12), 154.0 (s, fluorine-C10, C13), 162.4

(22) Straub, B.; Rominger, F.; Hofmann, P. *Inorg. Chem. Commun.* **2000**, 3, 214.

(23) Huang, D.; Streib, W. E.; Bollinger, J. C.; Caulton, K. G.; Winter, R. F.; Scheiring, T. *J. Am. Chem. Soc.* **1999**, 121, 8087.

(24) Rickard, C. E. F.; Roper, W. R.; Taylor, G.; Waters, J. M.; Wright, L. J. *J. Organomet. Chem.* **1990**, 389, 375.

(25) Holm, R. *Inorg. Synth.* **1970**, 12, 238.

(26) Moss, R. A.; Joyce, M. A. *J. Am. Chem. Soc.* **1978**, 100, 4475.

(t , $J_{PC} = 2.5$ Hz, pyridine-C2, C6), 316.8 (s, Ru=C). Anal. Calcd for $C_{36}H_{51}NP_2Cl_2Ru + C_4H_{10}O$: C, 59.62; H, 7.63. Found: C, 59.54; H, 7.68.

Synthesis of $[Ru\{=C(C_{12}H_8)\}Cl\{^iBu-PNP\}](BF_4)$, **2.** (a) To a solution of **1** (72 mg, 0.1 mmol) in THF (10 mL) was added $AgBF_4$ (19.5 mg, 0.1 mmol), and the mixture was stirred at room temperature for 0.5 h protected from light. After filtration, the dark yellow solution was evaporated to dryness under vacuum. The dark orange solid, complex **2**, was washed with diethyl ether (3×2 mL) and dried under vacuum for several hours (77 mg, 99%). (b) To a solution of **1** (36 mg, 0.05 mmol) in dioxane (10 mL) was added HBF_4 (50 μ L, 1 M in dioxane) at room temperature. The dark orange solution was stirred at room temperature for 1 h and evaporated to dryness under vacuum. The solid residue was dissolved in a minimum amount of THF (1 mL), followed by addition of diethyl ether (10 mL), which caused precipitation of a solid. The solid was isolated by filtration and dried under vacuum for several hours, yielding complex **2** as a dark orange solid (69 mg, 90%). $^{31}P\{^1H\}$ NMR (C_6D_6): 67.6 (s). 1H NMR (C_6D_6): 0.84 (t, 18H, $J_{PH} = 7.0$ Hz, $P(C(CH_3)_3)$), 1.33 (t, 18H, $J_{PH} = 7.1$ Hz, $P(C(CH_3)_3)_2$), 3.53 (dt, 2H, $J_{HH} = 17.3$ Hz, $J_{PH} = 4.5$ Hz, $-CHHP$), 4.30 (dt, 2H, $J_{HH} = 17.5$ Hz, $J_{PH} = 5.3$ Hz, $-CHHP$), 7.06 (t, 2H, $J_{HH} = 7.5$ Hz, fluorine-H2, H7), 7.36 (d, 2H, $J_{HH} = 7.5$ Hz, fluorene-H4, H5), 7.50 (d, 2H, $J_{HH} = 8.0$ Hz, pyridine-H3, H5), 7.59 (t, 2H, $J_{HH} = 7.5$ Hz, fluorene-H3, H6), 7.76 (t, 1H, $J_{HH} = 8.0$ Hz, pyridine-H4), 9.62 (d, 2H, $J_{HH} = 8.0$ Hz, fluorene-H1, H8). $^{13}C\{^1H\}$ NMR (C_6D_6): 28.8 (s, $P(CH(CH_3)_2)_2$), 30.9 (s, $P(C(CH_3)_3)_2$), 38.0 (s, $P(C(CH_3)_3)_2$), 39.0 (s, CH_2P), 120.0 (s, fluorine-C4, C5), 132.3 (s, pyridine-C3, C5), 132.9 (s, fluorine-C2, C7), 136.8 (s, fluorine-C3, C6), 140.5 (s, fluorine-C1, C8), 141.5 (s, pyridine-C4), 148.2 (s, fluorine-C11, C12), 151.4 (s, fluorine-C10, C13), 168.8 (s, pyridine-C2, C6), 299.9 (s, Ru=C). $^{19}F\{^1H\}$ NMR (C_6D_6): -149.0 (s). Anal. Calcd for $C_{36}H_{51}BNF_4P_2Cl_2Ru + CH_2Cl_2$: C, 51.20; H, 6.16. Found: C, 51.28; H, 6.13.

Synthesis of $[Ru\{=C(C_{12}H_8)\}Cl\{^iBu-PNP\}Cl]$, **3.** A solution of **1** (36 mg, 0.05 mmol) in toluene (15 mL) was heated at $110^\circ C$ for 8 h. After cooling to room temperature, the dark red solution was evaporated under vacuum and the solid residue was dissolved in a minimum amount of CH_2Cl_2 (1 mL). Upon addition of diethyl ether (15 mL) a solid precipitated and was isolated by filtration. After drying under vacuum for several hours, complex **3** was obtained as dark red solid (64 mg, 90%).

$^{31}P\{^1H\}$ NMR (CD_2Cl_2): 66.3 (s). 1H NMR (CD_2Cl_2): 1.07 (t, 18H, $J_{PH} = 7.2$ Hz, $P(C(CH_3)_3)$), 1.52 (t, 18H, $J_{PH} = 7.5$ Hz, $P(C(CH_3)_3)_2$), 3.47 (dt, 2H, $J_{HH} = 17.5$ Hz, $J_{PH} = 5.0$ Hz, $-CHHP$), 4.11 (dt, 2H, $J_{HH} = 17.5$ Hz, $J_{PH} = 5.0$ Hz, $-CHHP$), 5.78 (d, 1H, $J_{HH} = 7.5$ Hz, fluorine-C1 or C8), 6.89 (t, 1H, $J_{HH} = 7.5$ Hz, fluorine-C2, or C7), 7.22 (t, 1H, $J_{HH} = 7.5$ Hz, fluorine-H2 or H7), 7.41 (d, 2H, $J_{HH} = 7.5$ Hz, fluorene-H4, H5), 7.50 (t, 1H, $J_{HH} = 7.5$ Hz, fluorine-H3 or H6), 7.67 (t, 1H, $J_{HH} = 7.5$ Hz, fluorene-H3 or H6), 8.00 (d, 2H, $J_{HH} = 8.0$ Hz, pyridine-H3, H5), 8.17 (t, 1H, $J_{HH} = 8.0$ Hz, pyridine-H4), 8.98 (d, 1H, $J_{HH} = 7.5$ Hz, fluorene-H1 or H8). $^{13}C\{^1H\}$ NMR (CD_2Cl_2): 28.7 (s, $P(CH(CH_3)_2)_2$), 30.6 (s, $P(C(CH_3)_3)_2$), 38.3 (s, $P(C(CH_3)_3)_2$), 39.2 (s, CH_2P), 124.1 (s, fluorine-C4, C5), 127.7 (s, pyridine-C3, C5), 132.8 (s, fluorine-C2, C7), 136.5 (s, fluorine-C3, C6), 140.6 (s, fluorine-C1, C8), 141.7 (s, pyridine-C4), 147.9 (s, fluorine-C11, C12), 151.1 (s, fluorine-C10, C13), 168.5 (s, pyridine-C2, C6), 300.8 (s, Ru=C). Anal. Calcd for $C_{36}H_{51}NP_2Cl_2Ru$: C, 59.09; H, 7.03. Found: C, 59.18; H, 7.10.

Synthesis of $Ru\{N_2=C(C_{12}H_8)\}Cl_2\{^iBu-PNP\}$, **5.** To a solution of **4** (58 mg, 0.05 mmol) in toluene (15 mL) was added 9-diazofluorene (19 mg, 0.1 mmol) at $-32^\circ C$. The black-yellow solution was stirred at room temperature for 1 h and then evaporated to dryness under vacuum. The residue was dissolved in a minimal amount of benzene (1 mL), and pentane (10 mL) was added to

precipitate a black-blue solid, which was filtered off and dried under vacuum for several hours to obtain complex **5** (70 mg, 91%).

$^{31}P\{^1H\}$ NMR (C_6D_6): 65.8 (s). 1H NMR (C_6D_6): 1.43 (br t, 36H, $J_{PH} = 5.5$ Hz, $P(C(CH_3)_3)$), 3.94 (br s, 4H, $-CH_2P$), 6.56 (d, 2H, $J_{HH} = 8.0$ Hz, pyridine-H3, H5), 6.87 (t, 1H, $J_{HH} = 8.0$ Hz, pyridine-H4), 7.26 (t, 2H, $J_{HH} = 7.5$ Hz, fluorene-H3, H6), 7.48 (t, 2H, $J_{HH} = 7.5$ Hz, fluorine-H2, H7), 8.04 (d, 2H, $J_{HH} = 7.5$ Hz, fluorene-H4, H5), 8.22 (d, 2H, $J_{HH} = 7.5$ Hz, fluorene-H1, H8). $^{13}C\{^1H\}$ NMR (C_6D_6): 31.5 (s, $P(C(CH_3)_3)_2$), 35.8 (s, $P(C(CH_3)_3)_2$), 38.7 (s, CH_2P), 67.8 (s, fluorine-C9), 119.7 (s, fluorine-C4, C5), 120.4 (s, pyridine-C3, C5), 120.8 (s, fluorine-C2, C7), 123.1 (s, fluorine-C3, C6), 123.4 (s, fluorine-C1, C8), 126.1 (s, fluorine-C11, C12), 130.6 (s, fluorine-C10, C13), 134.3 (s, pyridine-C4), 166.7 (s, pyridine-C2, C6). IR (KBr pellets): 2054 cm^{-1} (ν_{N-N}). Anal. Calcd for $C_{36}H_{51}N_3P_2Cl_2Ru$: C, 56.91; H, 6.77. Found: C, 56.67; H, 6.30.

Synthesis of $[RuI_2(^iBu-PNP)]$, **6.** To a solution of complex **4b** (58 mg, 0.05 mmol) in acetone/THF (20 mL, 1:1 v/v) was added NaI (30 mg, 0.2 mmol) at room temperature. The mixture was stirred at room temperature for 24 h and filtered, and the filtrate was evaporated to dryness under vacuum. The residue was washed with diethyl ether (3×5 mL) and the resulting black-green solid was dried under vacuum for several hours to give 60 mg (80% yield) of complex **6**.

$^{31}P\{^1H\}$ NMR (acetone- d_6): 45.0 (s). 1H NMR (acetone- d_6): 0.71 (br s, 18H, $P(C(CH_3)_3)_2$), 1.68 (br s, 18H, $P(C(CH_3)_3)_2$), 4.30 (t, 4H, $J_{PH} = 3.8$ Hz, $-CH_2P$), 7.45 (t, 1H, $J_{HH} = 7.5$ Hz, pyridine-H4), 7.62 (d, 2H, $J_{HH} = 7.5$ Hz, pyridine-H3, H5). $^{13}C\{^1H\}$ NMR (acetone- d_6): 29.7 (br s, $P(CH(CH_3)_2)_2$), 32.6 (br s, $P(C(CH_3)_3)_2$), 38.7 (s, CH_2P), 120.4 (s, pyridine-C3, C5), 134.6 (s, pyridine-C4), 170.7 (s, pyridine-C2, C6). Anal. Calcd for $C_{23}H_{43}NP_2I_2Ru$: C, 36.81; H, 5.78. Found: C, 36.97; H, 5.71.

Reaction of Complex **4 with 2 equiv of $NaB(Et)_3H$.** A solution of **4** (11.6 mg, 0.01 mmol) in dry THF (2 mL) was cooled to $-32^\circ C$, followed by addition of 40 μ L of a solution of $NaB(Et)_3H$ (0.04 mmol, 1 M in toluene) at $-32^\circ C$. The mixture was kept at $-32^\circ C$ for 1 h, followed by stirring at room temperature for 2 h. The solution was filtered and its NMR measured. $^{31}P\{^1H\}$ NMR: 102.1 (s). 1H NMR: -4.6 (t, $J_{PH} = 22.5$ Hz, 2H), $t_1 = 1.20$ s. This solution is stable at room temperature for several hours and completely decomposed after 24 h. Trying to isolate this complex resulted in a mixture.

Synthesis of $[RuH(N_2)(PNP)(NHNC_{13}H_8)]$, **7.** A solution of **4** (11.6 mg, 0.01 mmol) in dry THF (2 mL) was cooled to $-32^\circ C$; then 40 μ L of a solution of $NaB(Et)_3H$ (0.04 mmol, 1 M in toluene) was added at $-32^\circ C$. The mixture was kept at $-32^\circ C$ for 1 h and then was stirred at room temperature for 2 h and filtered. To the yellow filtrate was added 9-diazofluorene (4 mg, 0.02 mmol), and the dark yellow solution was stirred at room temperature for 2 h. The solution was concentrated to 0.5 mL, and 5 mL of diethyl ether was slowly added. The mixture was kept at $-32^\circ C$ for 12 h, and the orange solid thus formed was isolated by filtration, washed with diethyl ether (3×1 mL), and dried under vacuum, to give 8 mg (57%) of complex **7**.

$^{31}P\{^1H\}$ NMR (THF- d_8): 81.0 (s). 1H NMR (THF- d_8): -12.01 (t, 1H, $J_{PH} = 19.0$ Hz, Ru-H), 1.28 (t, 18H, $J_{PH} = 6.5$ Hz, $P(C(CH_3)_3)$), 1.37 (t, 18H, $J_{PH} = 6.5$ Hz, $P(C(CH_3)_3)_2$), 3.45 (dt, 2H, $J_{HH} = 16.5$ Hz, $J_{PH} = 3.8$ Hz, $-CHHP$), 3.89 (br d, 2H, $J_{HH} = 16.5$ Hz, $-CHHP$), 6.80 (t, 1H, $J_{HH} = 7.5$ Hz, $J_{HH} = 7.0$ Hz), 6.89 (t, 1H, $J_{HH} = 7.5$ Hz, $J_{HH} = 7.0$ Hz), 6.98 (t, 1H, $J_{HH} = 7.5$ Hz), 7.11 (t, 1H, $J_{HH} = 7.5$ Hz, $J_{HH} = 7.0$ Hz) (fluorene-H2, H3, H6, or H7), 7.10 (d, 1H, $J_{HH} = 7.5$ Hz), 7.66 (d, 1H, $J_{HH} = 7.5$ Hz), 7.82 (d, 1H, $J_{HH} = 7.0$ Hz), 8.07 (d, 1H, $J_{HH} = 7.0$ Hz) (fluorene-H1, H4, H5, H8), 7.33 (d, 2H, $J_{HH} = 8.0$ Hz, pyridine-H3, H5), 7.61 (t, 1H, $J_{HH} = 8.0$ Hz, pyridine-H4), 9.15 (br s, 1H, HNN). $^{13}C\{^1H\}$ NMR (THF- d_8): 29.9 (br s, $P(CH(CH_3)_2)_2$), 30.3 (t, $J_{PC} = 2.5$ Hz, $P(CH(CH_3)_2)_2$), 36.0 (t, $J_{PC} = 10.1$ Hz, $P(C$

(CH₃)₃)₂, 36.9 (t, J_{PC} = 6.9 Hz, CH₂P), 38.0 (t, J_{PC} = 5.0 Hz, P(C(CH₃)₃)₂), 67.9 (s, C=N=N), 117.2 (s), 118.3 (s), 118.9 (s), 119.4 (s), 119.8 (s), 120.9 (s), 125.0 (s), 125.7 (s) (fluorine-C1, C2, C3, C4, C5, C6, C7, or C8), 120.3 (t, J_{PC} = 4.4 Hz, pyridine-C3, C5), 136.8 (s, pyridine-C4), 130.0 (s), 130.9 (s), 134.3 (s), 140.9 (s) (fluorine-C10, C11, C12, or C13), 166.4 (t, J_{PC} = 5.7 Hz, pyridine-C2, C6). IR (KBr pellets): 3205 cm⁻¹ (ν_{NN}), 2083 cm⁻¹ (ν_{NN}). Anal. Calcd for C₃₆H₅₃N₃P₂Ru: C, 60.15; H, 7.43; N, 9.73. Found: C, 60.24; H, 7.40; N, 9.20.

Synthesis of [PNPRu(NHNC₁₃H₇)], **8.** A solution of **7** (13.8 mg, 0.02 mmol) in dry THF (2 mL) was heated at 65 °C for 1 h and then cooled to room temperature. The dark red solution was concentrated to 0.5 mL, and diethyl ether (2.5 mL) was slowly added. The mixture was kept at -32 °C for 12 h, and the dark red solid that was formed was isolated by filtration, washed with diethyl ether (3 × 1 mL), and dried under vacuum to give 12.4 mg of complex **8** (90% yield).

³¹P{¹H} NMR (THF-*d*₈): 58.5 (s). ¹H NMR (THF-*d*₈): 0.70 (br s, 18H, P(C(CH₃)₃)₃), 1.20 (br s, 18H, P(C(CH₃)₃)₂), 3.49 (br d, 2H, J_{HH} = 17.4 Hz, -CHHP), 3.65 (br d, 2H, J_{HH} = 17.4 Hz, -CHHP), 5.71 (d, 1H, J_{HH} = 7.5 Hz), 6.95 (d, J_{HH} = 7.2 Hz), 7.62 (d, J_{HH} = 7.2 Hz), 7.75 (d, J_{HH} = 7.2 Hz) (fluorine-H2, H4, H5, or H8) 5.96 (t, J_{HH} = 7.2 Hz), 6.81 (t, 1H, J_{HH} = 8.2 Hz), 6.97 (t, 1H, J_{HH} = 7.2 Hz, J_{HH} = 8.2 Hz, fluorine-H3, H6, or H7), 7.40 (d, 2H, J_{HH} = 8.0 Hz, pyridine-H3, H5), 7.51 (t, 1H, J_{HH} = 8.0 Hz, pyridine-H4), 8.50 (br s, 1H, NH). ¹³C{¹H} NMR (THF-*d*₈): 29.4 (br s, P(CH(CH₃)₂)₂), 30.3 (br s, P(CH(CH₃)₂)₂), 36.3 (br s, CH₂P), 37.0 (br s, P(C(CH₃)₃)₂), 38.1 (br s, P(C(CH₃)₃)₂), 67.9 (br s, C=N=N), 112.3 (s), 116.1 (s), 117.5 (s), 119.1 (s), 119.2 (s), 123.0 (s), 128.3 (s) (fluorine-C2, C3, C4, C5, C6, C7, or C8), 120.9 (s, pyridine-C3, C5), 133.0 (s, pyridine-C4), 129.7 (s), 133.6 (s), 134.8 (s), 138.9 (s) (fluorine-C10, C11, C12, or C13), 158.4 (s, fluorine-C1), 167.8 (s, pyridine-C2, C6). Anal. Calcd for C₃₆H₅₁N₃P₂Ru: C, 62.77; H, 7.47. Found: C, 62.60; H, 7.55.

X-ray Crystal Structure Determination of Complexes 1, 2, 5, 6, and 8. The crystals were mounted on a nylon loop and flash frozen in a nitrogen stream at 120 K. Data were collected on a Nonius Kappa CCD diffractometer mounted on a FR590 generator equipped with a sealed tube with Mo K α radiation (λ = 0.71073 Å) and a graphite monochromator. Data were processed with Denzo-Scalepack. The five structures were solved using direct methods with SHELXS-97 and refined by full matrix least-squares based on F^2 .

Complex 1: C₃₆H₅₁NP₂Cl₂Ru + C₄H₁₀O, orange plate, 0.10 × 0.05 × 0.02 mm³, triclinic, $P\bar{1}$ (No. 2), a = 12.274(3) Å, b = 12.697(3) Å, c = 13.241(3) Å, α = 85.74(3)°, β = 81.89(3)°, γ = 83.86(3)°, V = 2027.5(10) Å³, Z = 2, fw = 805.8, $F(000)$ = 848, D_c = 1.320 Mg/m³, μ = 0.628 mm⁻¹. The final cycle of refinement based on F^2 gave an agreement factor R = 0.076 for data with $I >$

$2\sigma(I)$ and R = 0.098 for all data (4052 reflections) with a goodness-of-fit of 1.096. Idealized hydrogen atoms were placed and refined in the riding mode.

Complex 2: C₃₆H₅₁BNF₄P₂ClRu + CH₂Cl₂, yellow plate, 0.10 × 0.04 × 0.04 mm³, monoclinic, $P2(1)/c$, a = 16.659(1) Å, b = 15.011(1) Å, c = 16.473(1) Å, β = 109.116(4)°, V = 3892.2(4) Å³, Z = 4, fw = 868.0, $F(000)$ = 1792, D_c = 1.481 Mg/m³, μ = 0.738 mm⁻¹. The final cycle of refinement based on F^2 gave an agreement factor R = 0.047 for data with $I >$ $2\sigma(I)$ and R = 0.062 for all data (3955 reflections) with a goodness-of-fit of 1.054. Idealized hydrogen atoms were placed and refined in the riding mode.

Complex 5: C₃₆H₅₁N₃P₂Cl₂Ru, black plate, 0.30 × 0.10 × 0.05 mm³, orthorhombic, $Pbca$ (No. 61), a = 18.0783(3) Å, b = 14.7973(3) Å, c = 27.1111(6) Å, V = 7252.2(2) Å³, Z = 8, fw = 759.7, $F(000)$ = 3168, D_c = 1.392 Mg/m³, μ = 0.697 mm⁻¹. The final cycle of refinement based on F^2 gave an agreement factor R = 0.046 for data with $I >$ $2\sigma(I)$ and R = 0.079 for all data (8326 reflections) with a goodness-of-fit of 1.049. Idealized hydrogen atoms were placed and refined in the riding mode.

Complex 6: C₂₃H₄₃NP₂I₂Ru, green prism, 0.10 × 0.10 × 0.05 mm³, monoclinic, $P2(1)/c$ (No. 14), a = 14.880(3) Å, b = 12.005(2) Å, c = 16.352(3) Å, β = 104.79(3)°, V = 2824(1) Å³, Z = 4, fw = 750.4, $F(000)$ = 1472, D_c = 1.765 Mg/m³, μ = 2.865 mm⁻¹. The final cycle of refinement based on F^2 gave an agreement factor R = 0.038 for data with $I >$ $2\sigma(I)$ and R = 0.052 for all data (6340 reflections) with a goodness-of-fit of 1.053. Idealized hydrogen atoms were placed and refined in the riding mode.

Complex 8: C₃₆H₅₁N₃P₂Ru + 0.5 THF + 0.25 pentane, orange prism, 0.10 × 0.10 × 0.05 mm³, monoclinic, $C2/c$ (No. 15), a = 34.707(7) Å, b = 14.668(3) Å, c = 17.259(4) Å, β = 117.57(3)°, V = 7788(3) Å³, Z = 8, fw = 742.8, $F(000)$ = 3084, D_c = 1.255 Mg/m³, μ = 0.515 mm⁻¹. The final cycle of refinement based on F^2 gave an agreement factor R = 0.054 for data with $I >$ $2\sigma(I)$ and R = 0.069 for all data (6908 reflections) with a goodness-of-fit of 1.096. Idealized hydrogen atoms were placed and refined in the riding mode.

Acknowledgment. Support of this work by the German-Israeli Project Cooperation (DIP) and by the Israel Science Foundation is gratefully acknowledged. J. Zhang thanks the Harry K. Stone Foundation for a Postdoctoral Fellowship. D. Milstein is the holder of the Israel Matz Professorial Chair of Organic Chemistry.

Supporting Information Available: CIF files containing X-ray crystallographic data for compounds **1**, **2**, **5**, **6**, and **8**. This material is available free of charge via the Internet at <http://pubs.acs.org>.

OM800294V